Low Temperature Physics/Fizika Nizkikh Temperatur, 2012, v. 38, No. 8, pp. 953–960

Radiolysis of astrophysical ices by heavy ion irradiation: destruction cross section measurement

A.L.F. de Barros[1], P. Boduch[2], A. Domaracka[2], H. Rothard[2], and E.F. da Silveira[3]

[1]*Departamento de Disciplinas Básicas e Gerais, CEFET-RJ, Av. Maracanã 229, 20271-110 Rio de Janeiro, RJ, Brazil*
E-mail: ana1barros@gmail.com

[2]*Centre de Recherche sur les Ions, les Matériaux et la Photonique (CEA/CNRS/ ENSICAEN/Université de Caen-Basse Normandie), CIMAP-CIRIL-Ganil, Boulevard Henri Becquerel, BP 5133, F-14070 Caen Cedex 05, France*
E-mail: rothard@ganil.fr

[3]*Departamento de Física, Pontifícia Universidade Católica do Rio de Janeiro, Rua Marquês de São Vicente 225, 22451-900, Rio de Janeiro, RJ, Brazil*

Received April 19, 2012

Many solar system objects, such as planets and their satellites, dust grains in rings, and comets, are known to either be made of ices or to have icy surfaces. These ices are exposed to ionizing radiation including keV, MeV and GeV ions from solar wind or cosmic rays. Moreover, icy dust grains are present in interstellar space and in particular in dense molecular clouds. Radiation effects include radiolysis (the destruction of molecules leading to formation of radicals), the formation of new molecules following radiolysis, the desorption or sputtering of atoms or molecules from the surface, compaction of porous ices, and phase changes. This review discusses the application of infrared spectroscopy FTIR to study the evolution of the chemical composition of ices containing the most abundant molecular species found in the solar system and interstellar medium, such as H_2O, CO, CO_2 and hydrocarbons. We focus on the evolution of chemical composition with ion fluence in order to deduce the corresponding destruction and formation cross sections. Although initial approach focused on product identification, it became increasingly necessary to work toward a comprehensive understanding of ice chemistry. The abundances of these molecules in different phases of ice mantles provide important clues to the chemical processes in dense interstellar clouds, and therefore it is of importance to accurately measure the quantities such as dissociation and formation cross sections of the infrared features of these molecules. We also are able to obtain the scaling of these cross sections with deposited energy.

PACS: **34.50.–s** Scattering of atoms and molecules;
61.80.–x Physical radiation effects, radiation damage;
33.20.Ea Infrared spectra;
82.30.Fi Ion-molecule, ion-ion, and charge-transfer reactions.

Keywords: ion irradiation, astrophysical ices, destruction cross sections.

1. Introduction

Most of the outer space is at temperatures in the order of 10 to 80 K. In these regions, and at these temperatures, gases formed by relatively simple molecules such as nitrogen (N_2), oxygen (O_2), water (H_2O), carbon monoxide (CO), carbon dioxide (CO_2), ammonia (NH_3) and methane (CH_4) condense to form ice, which can be observed in comets, on the surface of satellites of giant planets and in interstellar grain mantles. In space, the ices are exposed to ion irradiation (stellar winds and galactic cosmic rays) ranging from protons up to heavy ions such as Fe, with kinetic energies from keV to TeV. Such bombardment leads to fragmentation of molecules inside the ice samples, as well as sputtering and formation of new molecules. Infrared astronomy has led to the identification of various species existing within icy grain mantles in dense clouds. The two most abundant molecules in grain mantles identified to date are H_2O and CO (e.g., [1–5]). Limited observational evidence as well as theoretical and laboratory modeling indicate that carbon dioxide (CO_2) should also be an important component of interstellar ices [2,6]. The goal of

this paper is to describe briefly some of the experiments performed at GANIL (Grand Accelerateur National d'Ions Lourds, Caen, France). As part of a systematical study on effects induced by heavy ions, our collaboration has previously reported results on pure H_2O, CO, CO_2, HCOOH, NH_3, CH_3OH and CH_4 ices. Also, water mixtures such as: H_2O:CO_2, H_2O:CO, H_2O:NH_3, H_2O:H_2CO and H_2O:NH_3:CO ices were irradiated with MeV ions and CO, CO_2 with keV ions. In this work, only the dissociation cross-section results obtained for keV and MeV projectile energies are presented.

2. Experimental method

In a typical "cosmic-ice" radiation experiment, a sample consisting of the molecules of interest is prepared by condensation of a room-temperature vapor onto a pre-cooled substrate in a vacuum chamber. The substrate temperature is usually selected with the temperature of a specific astronomical environment in mind. In this section the experimental setup and procedures used for producing and analyzing astrophysical ice analogs are described.

2.1. Sample chamber

The vacuum system used to analyze the ice samples adequate for infrared transmission analysis has been described previously [7–9]. The infrared transmitting substrate (CsI) is mounted in the vacuum chamber and can be cooled down by a closed-cycle helium refrigerator to a temperature of ~ 14 K. Typical residual gas pressure was $2{\cdot}10^{-8}$ mbar. For each deposition system, the gas flow from a storage tank to the vacuum system was regulated by a variable leak valve. The sample-cryostat system can be rotated by 180° and fixed at three different positions to allow i) gas deposition, ii) FTIR measurement, and iii) perpendicular ion irradiation, as described in Fig. 1. The homogeneity of the ice samples produced with the deposition tubes was checked by varying the spot size of the infrared beam on the sample using the variable aperture in front of the infrared source of the spectrometer. Samples were found to be homogeneous within 10% inside a diameter of 1.2 cm.

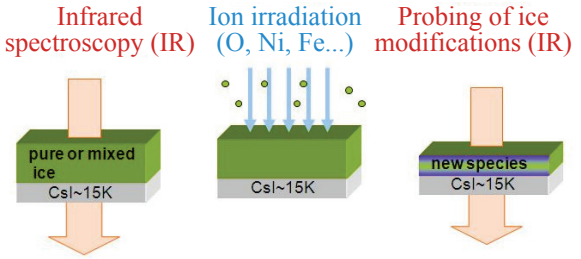

Fig. 1. Schematic diagram of the experimental procedure. The ion beam impinges perpendicularly on the thin ice film deposited on a CsI crystal.

2.2. FTIR analysis

The FTIR chamber was used at different GANIL beam lines: SME (≈ 10 MeV/u), IRRSUD (≈ 0.8 MeV/u) and ARIBE (≈ 1.6 keV/u). *In situ* analysis was performed by the Nicolet Fourier transform infrared spectrometer (FTIR) spectrometer (Magna 550) to obtain the spectrum in the 5000–600 cm^{-1} range with spectral resolution of 1 cm^{-1}. The molecular column density of a sample was determined from the relation between optical depth = ln (I_0 /I) and the band strength, A (cm/mol), of the respective sample vibration mode [6]. In this expression, I_0 and I are the intensity of light at a specific frequency before and after passing through a sample, respectively.

The Lambert–Beer equation was used for each spectrum on an optical depth scale by the relation for a different absorption $I(\nu) = I_0(\nu)\ \exp(-\varepsilon(\nu)N)$, in which $I(\nu)$ is the intensity of the IR beam after and $I_0(\nu)$ the before absorption at wavenumber ν. The $\varepsilon(\nu)$ is the wavenumber dependent absorption coefficient (in cm^2), and N is the column density (molecules per cm^2).

The absorption relation can also be expressed as a function of the absorbance:

$$A'(\nu) \equiv \log \frac{I_0(\nu)}{I(\nu)} = \frac{\varepsilon(\nu)N}{\ln 10}.$$

For normal IR incidence, integration of $A'(\nu)$ over the band width $\nu_f - \nu_i$ gives

$$N = \ln 10 \frac{\int_{\nu_i}^{\nu_f} A'(\nu)\, d\nu}{A}, \qquad (1)$$

where A is the integral absorption coefficient (in centimeter per molecule), referred here as "A-value".

3. Selected results

We first consider frozen water, hydrocarbons, and then carbon oxides, all important constituents of solar system and interstellar ices. In each case, typical radiation chemical alterations are described, i.e., giving quantitatively the cross sections obtained for each one.

3.1. H_2O *and hydrocarbon experiments*

Water is the dominant ice molecule in many astronomical environments, and so it is important to treat its radiation chemistry. On encountering either a high-energy ion or an energetic secondary electron, water molecules will be either ionized or electronically excited. These events give rise to a set of primary products that include charged species, radicals, and closed-shell molecules. Figure 2 shows FTIR spectra of water before and after irradiation. As we can see, under ion irradiation of the amorphous ice, the spectrum scarcely changes, except for a band that appears

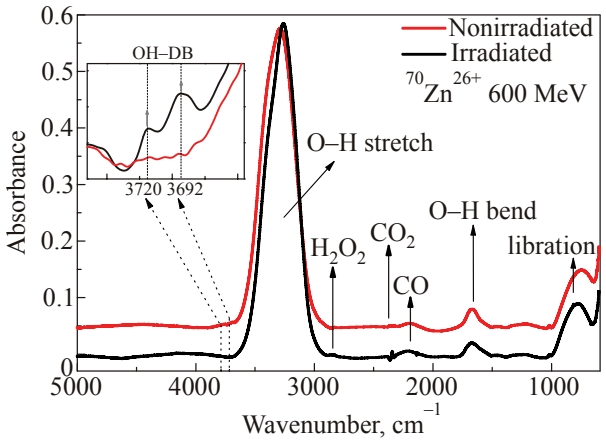

Fig. 2. Infrared spectra of condensed water at 13 K (amorphous ice) before and after irradiation with 600 MeV Zn^{26+} beam.

near 2850 cm^{-1}, the other features are water bands or due to some CO and CO_2 contamination. Figure 2 shows an enlargement of the relevant region, before (fluence zero) and after irradiation (high fluence). The band near 2850 cm^{-1} is due to H_2O_2 molecules [10], which we have confirmed by comparison with frozen H_2O_2 solutions. Although H_2O_2 has been a known radiolysis product of liquid H_2O for almost a century [11], the spectrum obtained after irradiation in Fig. 2 constitutes its first *in situ* observation of irradiated H_2O ice with 600 MeV Zn^{26+} beam. The accepted mode of H_2O_2 formation is combination of OH radicals, also observed by Moore *et al*. [12] and Boduch *et al*. [13]:

$$OH + OH = H_2O_2 . \qquad (2)$$

Our work on H_2O was motivated by the detection of a 2860 cm^{-1} feature on Europa's icy surface [14], in which H_2O_2 was assigned. Jovian magnetospheric radiation striking Europa dissociates H_2O ice into H and OH, and the above OH–OH reaction will follow. Another example of the formation of a radical, and its subsequent reaction, is provided by CH_4, methane. Irradiated CH_4 ice has been studied by several groups [15,16] and is of interest because it is constituent of both a solar system and an interstellar ices. Figure 3 shows IR spectra of CH_4 ice before and after irradiation at 16 K. Radiolysis leads the formation of the methyl radical, CH_3, which is indicated in Fig. 3,*a* with an arrow. For example, the combination of methyl radicals by

$$CH_3 + CH_3 = C_2H_6 \qquad (3)$$

gives C_2H_6, ethane, which can be identified in the Fig. 3 from many peaks for the irradiation by 220 MeV $^{16}O^{7+}$ beam. The remaining features are due to other hydrocarbon products and can be identified by reference spectra of various alkanes, alkenes, and alkynes. These examples involving H_2O and CH_4 were part of efforts to understand the radiation chemistry of saturated and unsaturated hydrocarbons in H_2O ice. An important aspect of this work is the investigation of H atom and OH radical addition reactions

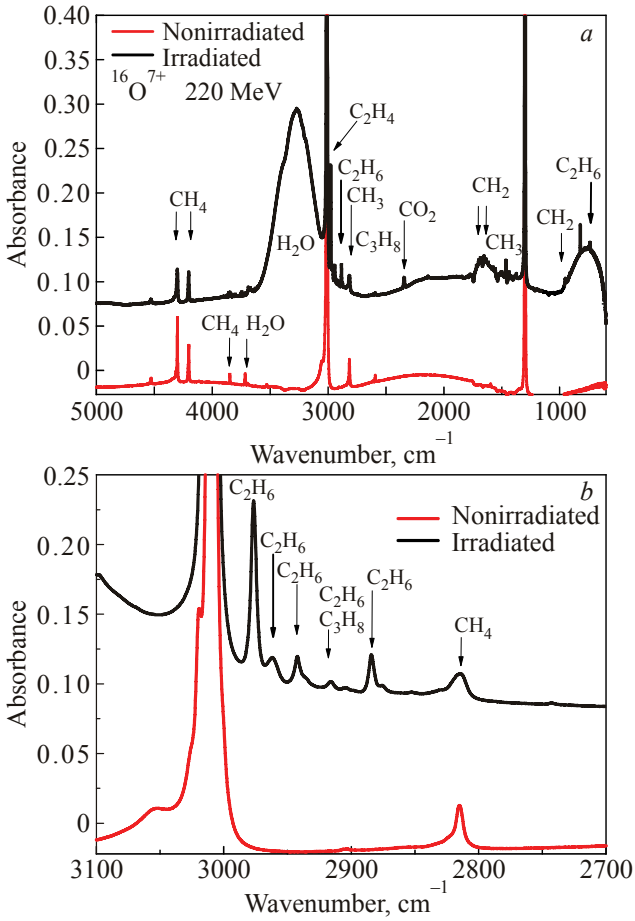

Fig. 3. Comparison of FTIR spectra regions of the CH_4 ice at 15 K before (lower) and after (upper) 220 MeV oxygen ion beam irradiation [18]. The spectrum corresponds to a final fluence of $4.29 \cdot 10^{13}$ ions/cm^2: ranges of 600–5000 cm^{-1} (*a*) and 2700–3100 cm^{-1} (*b*).

to carbon–carbon double and triple bonds. Specifically, the discovery of abundant C_2H_6 in comet C/1996 B2 Hyakutake by Mumma *et al*. [17] led them to suggest H atom addition to C_2H_2, acetylene, as a source of C_2H_6. We have confirmed that the sequence [18]:

$$C_2H_2 \rightarrow C_2H_4 \rightarrow C_2H_6 \qquad (4)$$

does occur at frozen temperatures thought to characterize comets stored in the Oort cloud [19,20].

Another important example is methanol. Methanol (CH_3OH) is the simplest organic alcohol; it is an important precursor of more complex pre-biotic species and its presence in several astrophysical environments has been reported [21]. The methanol was irradiated by four different ions beams: 16 MeV $^{16}O^{5+}$, 220 MeV $^{16}O^{7+}$, 600 MeV $^{65}Zn^{26+}$, and 770 MeV $^{86}Kr^{31+}$ ions (i.e., $v^2 \sim 1$, ~ 44, ~ 14, and ~ 10 MeV/u ions, respectively). The FTIR spectrum obtained from a pure CH_3OH sample was similar to previous studies [22].

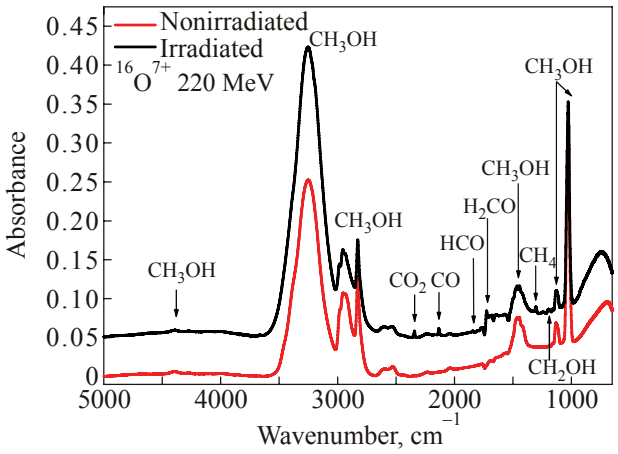

Fig. 4. Comparison of the infrared spectra of the methanol ice at 15 K, before irradiation (lower line) and after irradiation fluence of $2{\cdot}10^{13}$ ions/cm^2 for 220 MeV $^{16}O^{7+}$ ion beam [27].

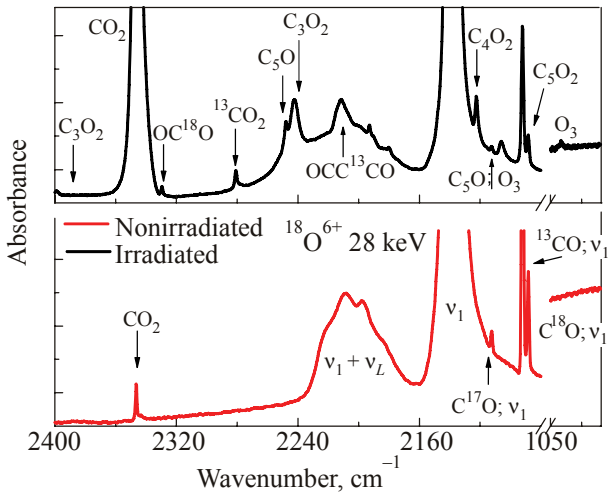

Fig. 5. Infrared spectrum of CO ice before and after 28 keV $^{18}O^{6+}$ irradiation [9] with a fluence of $1.17{\cdot}10^{13}$ ions/cm^2.

Segments of typical spectra are shown in Fig. 4, for oxygen ion beam. The 800–5000 cm^{-1} range of infrared spectra of the methanol ice at 15 K are shown, before irradiation (lower) and after irradiation (upper). The CO_2 band appears at 2342 cm^{-1}, and C_3O_2 occurs in two bands: ν_1 at 2193 cm^{-1} and ν_3 at 2233 cm^{-1} [23]. The band at 2233 cm^{-1} [24,25] is attributed to H_2O before irradiation. The CO band appears at 2136 cm^{-1}. The formation of H_2CO at 1720 cm^{-1} [22–26] is also observed. Finally, the peaks CH_4 at 1304 cm^{-1}, and $C_2H_4(OH)_2$ (ethylene glycol) at 1090 cm^{-1} [26] are visible. In addition, a weak band is visible near 1160 cm^{-1} which we attribute to CH_3OCHO.

3.2. CO *and* CO_2 *experiments*

The extremes of chemical oxidation for carbon are represented by hydrocarbons (reduced carbon) and carbon oxides. Having commented on hydrocarbon radiation chemistry, the radiation effects on the important ices CO and CO_2 are discussed.

Our investigation extends towards lower energy the analysis of the interaction of solar wind constituents with carbon monoxide ices present on the comet surfaces of the Oort cloud. This interaction is studied by bombarding a thin layer of CO with 28 keV $^{16}O^{6+}$ ions [9], an energy that is slightly above to that of the maximum abundance of solar wind distribution, as shown in Fig. 5. Before irradiation, the only molecular species present in the sample was carbon monoxide. Six optical absorptions were then identified: the fundamental stretching peak (ν_1) centered at 2136 cm^{-1}, the fundamental plus lattice vibration combination band ($\nu_1 + \nu_L$), 2208 cm^{-1} peak, the first overtone of the fundamental ($2\nu_1$) at 4251 cm^{-1}, the ^{13}C peak of the CO fundamental (ν_1) at 2091 cm^{-1}, and the $C^{18}O$ peak at 2088 cm^{-1}. One additional peak lies at 2112 cm^{-1}, which results from the vibrations of carbon monoxide molecules that are chemisorbed to the substrate. The C–O bond is weakened due to the antibonding $2\pi^*$ CO orbital resulting in weaker energy of vibration [9].

CO ices were also irradiated with Ni ions at high energy — 52 and 537 MeV. These results simulate the effects produced by high-energy heavy cosmic-ray ions in interstellar grain mantles [23,28]. The CO radiolysis effects induced by nickel ions, protons (200 keV [29,30]; 800 keV [24]); photons (10.2 eV [24,29,31,32]), and electrons (5 keV [33]) are quite similar.

3.3. Mixtures

A study on the interaction of heavier and energetic ions (46 MeV $^{58}Ni^{13+}$) with ammonia-containing ices H_2O:NH_3 (1:0.5), H_2O:NH_3:CO (1:0.6:0.4) [8] and (220 MeV $^{16}O^{7+}$) with H_2O:H_2CO (10:9, this ice also contained 5% of CH_3OH), were performed to simulate physical chemistry effects induced by heavy-ion cosmic rays inside dense astrophysical environments.

Mixtures of NH_3 and CO with water seem to have a similar dissociation rate [8], reaching half the initial values at a fluence of about 10^{12} ions/cm^2. It was observed that the column density of water decreases too slowly as the fluence increases. This is attributed to a persistent deposition of water from the residual gas. This effect was not observed in previous experiments for pure CO and CO_2 ices [7,23], being probably related to the deposition of water-containing ices; however, it was also observed in the mixture with H_2CO.

A recent and nonpublished experiment of the mixture H_2O:H_2CO irradiated with 220 MeV $^{16}O^{7+}$ ions (i.e., $v^2 \sim 14$ MeV/u ions at 15 K) is presented in Fig. 6. Several absorption bands due to molecular vibrations of H_2CO:H_2O before and after irradiation, are observed in the spectra of this figure. In Fig. 6,*a*, two entire infrared spectra of the H_2CO:H_2O ice are shown: before irradiation (lower spectra) and after irradiation (upper spectra). For

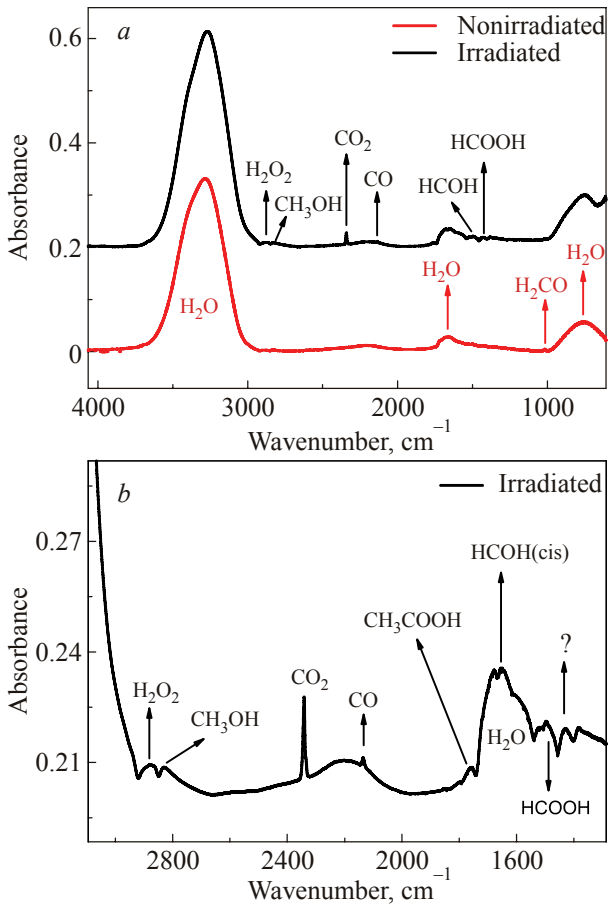

Fig. 6. (*a*) Comparison of the infrared spectra of the H_2O:H_2CO ice at 15 K, before (botton) and after irradiation with fluence of $2.1 \cdot 10^{13}$ ions/cm^2 by 220 MeV $^{16}O^{7+}$ ion beam (upper line). (*b*) A zoom of the irradiated sample spectrum at region 3100 to 1300 cm^{-1}.

water we observed three predominant bands: 3250 cm^{-1}, 1651 cm^{-1} and 760 cm^{-1}. Formaldehyde, H_2CO, could be identified via its fundamental 1249 cm^{-1} band, which is relatively isolated and has been used previously to constrain H_2CO production [22]. These bands were also identified by Gerakines *et al*. [31] as well as by Hudson & Moore [26]. In Fig. 6,*b* an expanded segment of the irradiated sample spectrum is presented. The CO_2 band is seen at 2342 cm^{-1} while CO band appears at 2138 cm^{-1}. In addition, an unknown weak band appears near 1384 cm^{-1}. The 2850 cm^{-1} band is attributed to H_2O_2 [34]. For methanol ice we notice a ν_3 band at 2827 cm^{-1} [27]; HCOH identified by the ν_4 — 1430 cm^{-1} band [22]. The band at 1738 cm^{-1} is due to the CHOH ν_{14} = HCOH (cis); HCO at 1853 cm^{-1} band [35] and a small peak around 1762 cm^{-1} that can be due to CH_3COOH [36] or $HCOCH_2OH$ [22]. The very small bands at 1072 cm^{-1} are attributed to HCOOH molecules [35].

The study of column density variation of synthesized molecules in H_2O:H_2CO mixtures shows that HCOOH is a small product of oxygen beam irradiation. We also observed that the destruction yield of H_2CO is much higher than that found by Moore *et al*. [37]. One possible explanation is the fact that, in their mixture, the concentration of H_2O was five times higher than H_2CO, and furthermore in our case very energetic ion beams were employed. Other molecular species such as CO, CH_3OH, HCOOH and the HCO it is possible to observe an interesting point: the abundance of all the species finished at the same value as with proton irradiation, except for CH_3OH that is one of the most abundant species that where destroyed with 220 MeV oxygen ions.

4. Destruction cross section

Initially, the sample is formed only by precursor molecules. As irradiation goes on, they may either be destroyed (dissociation) or be ejected (sputtering) by the projectile ions. The column density evolves with an exponential behavior, as can be seen for example in Fig. 7, for the case of CH_3OH. In the methanol experiment, seven CH_3OH optical absorptions bands were identified. Methanol can be observed by the infrared spectroscopy via many different transitions, such as: (i) a small band at 4393 cm^{-1} due to the OH stretching mode; (ii) a intense band centered at 3250 cm^{-1} OH due to a stretching mode (mixture with the water band); (iii) two weak bands at 2959 or 2627 cm^{-1} due to the combination mode of the CH stretch symmetric and asymmetric stretch mode, respectively; (iv) a 1457 cm^{-1} band due to CH_3 deformation modes; (v) a weak band at 1129 cm^{-1} is due to the CH_2 or CH_3 rock; and (vi) a very intense band at 1026 cm^{-1} is due to CO stretching mode [27].

The effects of ion irradiation on pure CH_3OH as a function of the column density and beam projectile fluence, for the 16 MeV $^{16}O^{5+}$, 220 MeV $^{16}O^{7+}$, 600 MeV $^{65}Zn^{26+}$ and 770 MeV $^{86}Kr^{31+}$ are shown in Fig. 8.

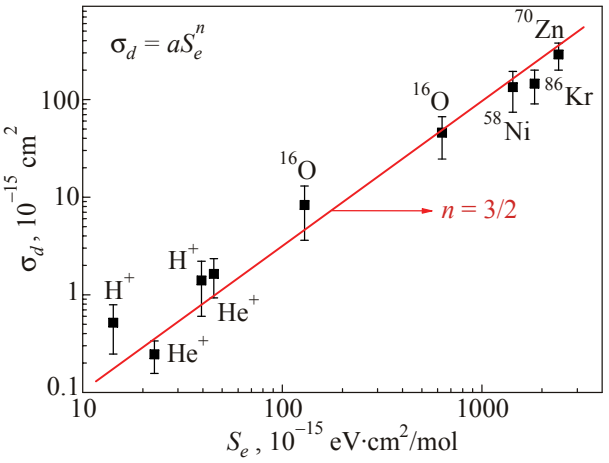

Fig. 7. The dependence of CH_3OH destruction cross section on the electronic stopping power. Data for 16 and 220 MeV O, Zn, and Kr are results of the de Barros *et al*. [27]. For lower energy beam see [25,41,42]. The lines correspond to the function $\sigma_d \sim S_e^n$, for 3/2 (solid line).

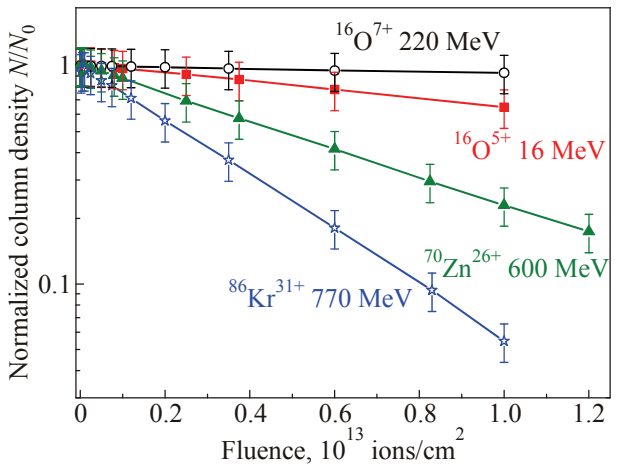

Fig. 8. Ion irradiation on pure CH_3OH as a function of the column density and beam projectile fluence, for the 16 MeV $^{16}O^{5+}$, 220 MeV $^{16}O^{7+}$, 600 MeV $^{65}Zn^{26+}$ and 770 MeV $^{86}Kr^{31+}$.

The determination of the destruction cross section σ_d of the precursor molecules can be obtained by a simple model. L_1 and Y_1 are defined as the layering and the sputtering yields, respectively; $\Omega_1(F)$ is the coverage of the precursor species (1) on the sample surface after the beam fluence F. N_j is the column density of molecular species i; σ_f and σ_d are their formation and destruction cross sections, respectively. Data evolution can be described by the system of differential equations [23]:

$$\frac{dN_1}{dF} = \sum_j \sigma_{f,1j} N_j + L_1 - \sigma_{d,i} N_1 - Y_1(0)\Omega_1(F). \qquad (5)$$

If no layering occurs during the irradiation and if no recombination takes place (i.e., the precursor molecule is not formed from its own fragments), then $L_1 = 0$ and $\sigma_{f,1j} = 0$. Moreover, since $\Omega_1(F)$ is proportional to $N_1(F)$, the solution of Eq. (5) is

$$N_1(F) = N_{1,0} \exp\left[-F\left(\sigma_{d,1} + \frac{Y_1(0)}{N_{1,0}}\right)\right]. \qquad (6)$$

Fitting the experimental data with this expression, the values of $N_{1,0}$ and of the sum $\sigma_{d,1} + Y_1(0)/N_{1,0}$ are determined, but not the $\sigma_{d,1}$ and $Y_1(0)$ values individually.

The occurrence of the layering (intentionally or not) of a gas distinct from the sample stops the sputtering (i.e., $Y_1(F) = Y_1(0) = 0$), which allows the σ_d determination unambiguously.

Table 1 lists the ices studied to date. In each case, their molecules were irradiated in H_2O ice, usually at a concen-

Table 1. Destruction cross sections for molecules at ~ 14 K, identified in related experiment

Molecule	Mixture H_2O:NH_3:CO:H_2CO:CO_2	Projectile / Energy	σ_d, 10^{-13} cm^2	Reference
CO	pure	52 MeV Ni^{13+}	1	[23] and [28]
	pure	537 MeV Ni^{24+}	0.3	[23] and [28]
	pure	28 keV $^{16}O^{6+}$	0.2	[9]
	(1:0.6:0.4:0:0)	46 MeV Ni^{11+}	1.9	[8]
	(1:0.6:0.4:0:0)	46 MeV Ni^{11+}	1.9	[8]
	(1:0.6:0.4:0:0)	46 MeV Ni^{11+}	1.9	[8]
CO_2	pure	46 MeV Ni^{11+}	1.7	[23] and [28]
	pure	52 MeV Ni^{13+}	1.8	[38]
	(1:0:0:0:1)	52 MeV Ni^{13+}	1.6	[38]
	(10:0:0:0:1)	52 MeV Ni^{13+}	~ 1	[38]
	(0:0:0:0:1)	28 keV $^{16}O^{6+}$	0.2	[9]
CH_4	pure	220 MeV O^{7+}	~ 0.04	[18]
H_2O	(1:0:1:0:0)	46 MeV Ni^{11+}	~ 2	[8]
	(1:0.5:0:0)	46 MeV Ni^{11+}	~ 2	[8]
	pure	52 MeV Ni^{13+}	1.1	[8]
	(10:0:0:0:1)	52 MeV Ni^{13+}	~ 1	[8]
	(1:0:0:0:1)	52 MeV Ni^{13+}	~ 10	[8]
	(1:0:0:1:0)	220 MeV O^{7+}	0.2	[39]
H_2CO	(1:0:0:1:0)	220 MeV O^{7+}	0.2	[39]
NH_3	(1:0.5:0:0:0)	46 MeV Ni^{11+}	1.3	[8]
	(1:0.6:0.4:0:0)	46 MeV Ni^{11+}	1.4	[8]
HCOOH	pure	267 MeV Fe^{22+}	1.4	[40]
CH_3OH	pure	220 MeV O^{7+}	0.2	[27]
	pure	16 MeV O^{5+}	~ 0.5	[27]
	pure	606 MeV Zn^{26+}	~ 1.4	[27]
	pure	774 MeV Kr^{31+}	~ 2.9	[27]

tration of 20% or less. IR spectra were taken and product identifications were made. The results of these experiments reveal the main products of radiation processing in each case and allow us to determine radiation lifetimes for various molecules.

5. Discussion and conclusions

The present experiments on radiation chemical effects led to a general observation that the destruction cross sections of heavy ions are ruled by a power law as a function of the electronic stopping power: $\sigma_d \sim S_e^n$. We show as example CH_3OH ice, for which literature data were included in the analysis (Fig. 8). For CH_3OH the n value was $\sim 3/2$. The main conclusion is that molecular destruction by fast ions is an over-linear phenomenon as a function of the transferred energy. High stopping power interactions are more efficient to dissociate the matrix molecules and also, as a consequence, to produce new chemical species. The same average value $n \sim 3/2$, was observed as well as in experiments with pure HCOOH [40], pure CH_4 ices [18], and in the mixture H_2O:H_2CO for the H_2CO molecule [39]. Measurements using other matrixes are being performed in order to verify if this law can be generalized.

Another interesting effect is that heavy ion radiation processing is very efficient in producing certain molecular species in ices. These species include CO, CO_2, CH_4, CH_3OH, and HCOOH. Each of these can be produced in sufficient yield from suitable laboratory precursors to account for observed abundances in many astronomical ices. A challenge for experimentalists is to determine the conditions under which the formation of such molecules might either be enhanced or hindered. In contrast to these "favored" molecules, we have found difficulties to detect other types. This occur in particular for molecules that are not seen by FTIR. These molecules may form part of the residual material already described, but such samples are not easily analyzed by conventional IR spectroscopy.

A useful concept in this kind of analysis is thermodynamic stability. Ionizing radiation drives the ice toward a more stable composition, reactants to products. However, if the experiment is repeated starting with the products, the original reactants are recovered as the ice approaches an equilibrium composition. Many examples can be given. Irradiation of CO in amorphous H_2O ice generates CO_2, CH_3OH, and the other products already described. However, irradiation of either H_2O:CO_2 or H_2O:CH_3OH ices generates CO. Some other pairs of reactants and products showing this behavior, all in H_2O matrix ices, are CO_2, H_2CO_3, CH_4, C_2H_6, CH_4, CH_3OH, H_2CO, CH_3OH and CO, H_2CO. This implies in multicomponent ices, such as H_2O:NH_3:CO and H_2O:H_2CO, that complex organic are formed by radiolysis in low yields. Conversely, it also implies that organic molecules, such as amino acids or organic polymers, are destroyed in H_2O ice by radiation, forming CO_2, NH_3, and other simple products. Turning from radiation products to radiation processes, it is observed that certain chemical reactions occur in a variety of molecules in H_2O-dominated ices. Double and triple bonds of types $C=C$, $C\equiv C$, $C=O$, and $C\equiv O$ are converted to single bonds by irradiation in H_2O ice [43]. Radical-radical reactions to make molecules like H_2O_2, C_2H_6, CH_3OH, and ethylene glycol [44] readily occur and are so common that they can be relied on in ices not yet studied. Nevertheless, the results obtained have shown that one key to understand complex ice chemistry is to start studying simple systems. Certainly there is a need to investigate and understand simple laboratory ices for comparisons to solar system and interstellar ices.

Once the behavior of individual molecules in the pure state is understood, one can turn to a radiation of a mixture for a reasonable set of chemical reactions and products. The situation that has existed up until now, in which each astronomical ice analogue studied represented a single chemical system, is changing as a comprehensive picture of energetic processing emerges.

Acknowledgments

This work was supported by the region of "Basse-Normandie" (France) and by the French-Brazilian exchange program CAPES-COFECUB. It is a pleasure to thank all the collaborators: E. Dartois, E. Seperuelo Duarte, S. Pilling, D. Andrade, V. Bordalo and also Th. Been and J.M. Ramillon, for technical support. The experiment was performed at the GANIL facility in Caen, France. The Brazilian agencies CNPq (INEspaço) and FAPERJ also provided partial support.

1. R. Smith, K. Sellgren, and A. Tokunaga, *Astrophys. J.* **344**, 413 (1989).
2. D. Whittet, A. Adamson, W. Duley, T. Geballe, and A. McFadzen, *Mon. Not. R. Astron. Soc.* **241**, 707 (1989).
3. D. Whittet, R. Smith, A. Adamson, D. Aitken, J. Chiar, T. Kerr, P. Roche, C. Smith, and C. Wright, *Astrophys. J.* **458**, 363 (1996).
4. A. Tielens, A. Tokunaga, T. Geballe, and F. Baas, *Astrophys. J.* **381**, 181 (1991).
5. J. Chiar, A. Tielens, D. Whittet, W. Schutte, A. Boogert, D. Lutz, E. Dishoeck, and M. Berstein, *Astrophys. J.* **537**, 749 (2000).
6. L. D'Hendecourt, L. Allamandola, R. Grim, and J. Greenberg, *Astron. Astrophys.* **158**, 119 (1986).
7. E. Seperuelo Duarte, P. Boduch, H. Rothard, T. Been, E. Dartois, L.S. Farenzena, and E.F. da Silveira, *Astron. Astrophys.* **502**, 599 (2009).
8. S. Pilling, E. Seperuelo Duarte, E.F. da Silveira, E. Balanzat, H. Rothard, A. Domaracka, and P. Boduch, *Astron. Astrophys.* **509**, A87 (2010).

9. A.L.F. de Barros, A. Domaracka, E. Seperuelo Duarte, P. Boduch, H. Rothard, and E.F. da Silveira, *Nucl. Instrum. Meth. Phys. Res.* **B269**, 852 (2011).
10. J. Lannon, F.D. Verderame, and R.W. Anderson, Jr., *J. Chem. Phys.* **54**, 2212 (1971).
11. M. Kernbaum, *Le Radium* **7**, 242 (1919).
12. M. Moore and R.L. Hudson, *Icarus* **154**, 282 (2000).
13. P. Boduch, E.F. da Silveira, A. Domaracka, O. Gomis, X. Lv, M. Palumbo, S. Pilling, H. Rothard, E. Seperuelo Duarte, and G. Strazzulla, *Adv. Astron.* **2011**, Article ID 327641 (2011).
14. R. Carlson, R. Johson, and M. Anderson, *Science* **286**, 97 (1999).
15. R. Kaiser and K. Roessler, *Astrophys. J.* **474**, 144 (1997).
16. G. Foti, L. Calcagno, K. Sheng, and G. Strazzulla, *Nature* **310**, 126 (1984).
17. M. Mumma, M.A. DiSanti, N.D. Russo, M. Fomenkova, K. Magee-Sauer, C.D. Kaminski, and D.X. Xie, *Science* **272**, 1310 (1996).
18. A.L.F. de Barros, V. Bordalo, E. Seperuelo Duarte, E.F. da Silveira, A. Domaracka, H. Rothard, and P. Boduch, *Astron. Astrophys.* **531**, 15 (2011).
19. R. Hudson and M.H. Moore, *Icarus* **126**, 233 (1997).
20. M. Moore and R.L. Hudson, *Icarus* **135**, 518 (1998).
21. K. Willacy and T. Millar, *Mon. Not. R. Astron. Soc*. **298**, 562 (1998).
22. C. Bennett, S.-H. Chen, B.-J. Sun, A. Chang, and R. Kaiser, *Astrophys. J.* **660**, 1588 (2007).
23. E. Seperuelo Duarte, A. Domaracka, P. Boduch, H. Rothard, E. Dartois, and E.F. da Silveira, *Astron. Astrophys.* **512**, A71 (2010).
24. P. Gerakines and M. Moore, *Icarus* **154**, 372 (2001).
25. P. Gerakines, M. Moore, and R. Hudson, *J. Geophys. Res.* **106**, 33381 (2001).
26. R. Hudson and M.H. Moore, *Icarus* **145**, 661 (2000).
27. A.L.F. de Barros, A. Domaracka, D.P.P. Andrade, P. Boduch, H. Rothard, and E.F. da Silveira, *Mon. Not. R. Astron. Soc*. **418**, 1363 (2011).
28. A. Domaracka, E. Seperuelo Duarte, P. Boduch, H. Rothard, J. Ramillon, S. Pilling, L.S. Farenzena, and E.F. da Silveira, *Nucl. Instrum. Meth. Phys. Res*. **B268**, 2960 (2010).
29. M. Loeffler, G.A. Barata, M. Palumbo, G. Strazulla, and R. Baragiola, *Astron. Astrophys.* **435**, 587 (2005).
30. M. Palumbo, G. Baratta, D. Fulvio, M. Garozzo, O. Gomis, G. Leto, F. Spinella, and G. Strazzulla, *J. Phys. Conf. Series* **101**, 01200 (2008).
31. P. Gerakines, W. Schutte, and P. Ehrenfreund, *Astron. Astrophys.* **312**, 289 (1996).
32. H. Cottin, M. Moore, and Y. Benilan, *Astrophys. J.* **590**, 874 (2003).
33. C. Jamieson, C. Bennett, A.M. Mebel, and R.I. Kaiser, *Astrophys. J.* **624**, 436 (2005).
34. M. Loeffler, U. Raut, R. Vidal, R. Baragiola, and R. Carlson, *Icarus* **180**, 265 (2006).
35. R. Hudson and M.H. Moore, *Icarus* **140**, 451 (1999).
36. S. Bisschop, J. Jorgensen, T. Bourke, S. Bottinelli, and E. van Dishoeck, *Astron. Astrophys.* **488**, 956 (2008).
37. M. Moore, R. Ferrante, R.L. Hudson, and J.N. Stone, *Icarus* **190**, 260 (2007).
38. S. Pilling, E. Seperuelo Duarte, A. Domaracka, H. Rothard, P. Boduch, and E.F. da Silveira, *Astron. Astrophys.* **523**, A77 (2010).
39. A.L.F. de Barros, *et al.*, In preparation.
40. D.P.P. Andrade, *et al.*, In preparation.
41. R. Brunetto, V. Orofino, and G. Strazzulla, *Mem. S. A. It. Suppl*. **6**, 45 (2005).
42. G.A. Baratta, G. Leto, and M.E. Palumbo, *Astron. Astrophys.* **384**, 343 (2002).
43. R. Hudson and M. Moore, *J. Geophys. Res.* **106**, 275 (2001).
44. R. Hudson, M.H. Moore, and P.A. Gerakines, *Astrophys. J.* **550**, 1140 (2000).